Hydrophobic nanoparticles improve permeability of cell-encapsulating poly(ethylene glycol) hydrogels while maintaining patternability

Wonjae Lee[a], Nam-Joon Cho[b], Anming Xiong[b], Jeffrey S. Glenn[b,c,1], and Curtis W. Frank[d,2]

[a]Department of Mechanical Engineering, Stanford University, Stanford, CA 94305; [b]Department of Medicine, Division of Gastroenterology and Hepatology, School of Medicine, Stanford University, Stanford, CA 94305; [c]Veterans Administration Medical Center, Palo Alto, CA 94304; and [d]Department of Chemical Engineering, Stanford University, Stanford, CA 94305

Edited by Chad A. Mirkin, Northwestern University, Evanston, IL, and approved October 13, 2010 (received for review April 19, 2010)

Cell encapsulating poly(ethylene glycol) hydrogels represent a promising approach for constructing 3D cultures designed to more closely approximate in vivo tissue environment. Improved strategies are needed, however, to optimally balance hydrogel permeability to support metabolic activities of encapsulated cells, while maintaining patternability to restore key aspects of tissue architecture. Herein, we have developed one such strategy incorporating hydrophobic nanoparticles to partially induce looser cross-linking density at the particle-hydrogel interface. Strikingly, our network design significantly increased hydrogel permeability, while only minimally affecting the matrix mechanical strength or prepolymer viscosity. This structural advantage improved viability and functions of encapsulated cells and permitted micron-scale structures to control over spatial distribution of incorporated cells. We expect that this design strategy holds promise for the development of more advanced artificial tissues that can promote high levels of cell metabolic activity and recapitulate key architectural features.

tissue engineering | cell encapsulation | hydrogel network properties | hepatitis C virus

Engineered tissues are expected to help overcome shortcomings associated with standard in vitro 2D culture and traditional tissue replacement therapies and provide an improved platform to study various biological assays (1). Several types of cells cultured as two-dimensional monolayers are known to dedifferentiate and lose their original functions due to disruption of their normal microenvironments (2). Thus, it has been a major challenge in the field of tissue engineering to provide structural and functional support equivalent to native tissues (3). Use of hydrogels as a scaffold material for engineered tissues has been of increasing interest due to their structural similarity to the extracellular components in the body (4). PEG is one of the most extensively utilized hydrogels because its network structure can be easily modified to mimic critical aspects of the original microenvironments (5). Various approaches to design PEG networks for improved phenotype stability of encapsulated cells have involved conjugating other biologically active factors to the polymer network and incorporating degradable linkages (6). Another advantage of PEG is that use of photolithography or microfluidic processing allows fabrication of microarchitectures that potentially recapitulate key aspects of tissue architecture to guide cells' behavior with respect to morphology, cytoskeletal structure, and functionality (7).

Beyond the restoration of its original microarchitecture, a three-dimensional matrix of an engineered tissue needs to provide sufficient permeability to support metabolic activities, provide for unimpeded transport of large macromolecules, and permit multiple cell-type interactions that are normally present in most original tissues (8). Even though the matrix diffusion condition could be gradually improved by promoting angiogenesis or conjugating degradable linkages (9), it is necessary to allow sufficient diffusion of substances indispensable to cell survival during the period immediately after cells are encapsulated (6). In addition, because many scaffolds for tissue engineering initially need to fill a space and provide a framework for the replaced tissue, the mechanical properties of the material are important (6). However, it is a challenge for hydrogel-based scaffolds to allow sufficient permeability while maintaining mechanical properties sufficient for generating and sustaining reconstructed tissue architectures. In many polymeric materials, improved permeability of networks has been obtained by increasing the distance between consecutive cross-links (10). This comes, however, at a cost of decreased mechanical strength in the resulting hydrogel network. Nevertheless, the traditional approach also results in increased viscosity of the liquid phase prepolymer, which retards flow of the prepolymer solution through micro-scale mold structures and also leads to decreased mechanical strength of the cured hydrogel. There have been attempts to address the relationship between the traditional polymeric parameters and the behavior of encapsulated cells in PEG networks (11). We recently determined that cell encapsulation leads to the formation of network defects and these network defects are up to orders of magnitude larger than the possible distance range between the network cross-links (12). In this work, we suggest that the level of these network defects is an appropriate spatial feature for tuning network permeability and patternability. We therefore attempted to augment network defects by incorporating hydrophobic poly(lactic-co-glycolic acid) (PLGA) nanoparticles (NPs) within the hydrophilic PEG network. This modification improved hydrogel permeability with minimum loss of patternability. Our network design led to improved viability and function of encapsulated human liver-derived cells and has the structural advantage of supporting micron-scale architectures for control of the spatial distribution of incorporated cells.

Results and Discussion

Augmentation of Network Defects by Incorporating Hydrophobic Nanoparticles Improves the Phenotype Stability of Encapsulated Cells. Because the viability of encapsulated liver-derived cells has been shown to be susceptible to the encapsulating matrix diffusion con-

Author contributions: W.L., N.-J.C., J.S.G., and C.W.F. designed research; W.L. and A.X. performed research; W.L. and N.-J.C. analyzed data; and W.L., N.-J.C., J.S.G., and C.W.F. wrote the paper.

The authors declare no conflict of interest.

This article is a PNAS Direct Submission.

Freely available online through the PNAS open access option.

[1]To whom correspondence may be addressed at: Division of Gastroenterology and Hepatology, School of Medicine, Stanford University, Center for Clinical Science Research Building, Room 3110, 269 Campus Drive, Stanford, CA 94305. E-mail: jeffrey.glenn@stanford.edu.

[2]To whom correspondence may be addressed at: Department of Chemical Engineering, Stanford University, 381 North-South Mall, Stauffer III, Stanford, CA 94305. E-mail: curt.frank@stanford.edu.

This article contains supporting information online at www.pnas.org/lookup/suppl/doi:10.1073/pnas.1005211107/-/DCSupplemental.

dition (13), we utilized human liver-derived cells as a model to evaluate the structure of cell-encapsulating PEG networks. Immortalized Huh 7.5 cells were chosen to optimize cell-encapsulating conditions prior to studies with human primary hepatocytes. Based on this scheme, we expanded upon recent work on the scale of network defects within a cell-encapsulating PEG hydrogel (12). In this previous work, we first encapsulated cells into PEG matrices and added virus particles into the cell culture medium (12). We then observed that encapsulated liver-derived cells could be infected with hepatitis C and pseudotyped lentiviruses, and the progeny of the viruses could be recovered from the media supernatants (12). The sizes of the hepatitis C virus (HCV) and the lentivirus particles are 50 nm and 100 nm, respectively. However, when the possible distances between consecutive cross-links are roughly estimated from uniformly cross-linked networks of 3.4 k or 8 k PEG, they cannot exceed 5 nm (14). We suggested that the cell-encapsulating PEG networks had numerous network defects large enough for the virus particles to successfully penetrate and infect the cells (12). Therefore, network defects appear to provide a major pathway for solute diffusion, such that the overall permeability would not be expected to be substantially improved by designing the network to have increased distances between the consecutive cross-links. To test this hypothesis, we measured cell viability in samples with either increased molecular weight of the polymer (e.g., 8 k vs. 3.4 k) or decreased solid content (e.g., 20% vs. 10%) as compared to the 20% 3.4 k PEG reference network. As shown in Fig. 1*A*, the results imply that all of the tested networks appeared to have similar levels of network defects to that of the reference as assessed by cell viability. The decreased viability in samples prepared with a further increase in solid content from 20% 3.4 k PEG (Fig. 1*B*) seems that fewer network defects were produced during polymerization, and the distances between consecutive cross-links determined the overall network permeability. Based on this understanding of the cell-encapsulating PEG network, we sought to augment the level of network defects to further improve the permeability.

It has been reported that hydrogels cured in contact with hydrophobic surfaces exhibit characteristics attributed to lower cross-linking density than hydrogels cured on hydrophilic glasses (15). The major driving force for inhomogeneous gelation adjacent to a hydrophobic surface is thought to be the high interfacial energy between the hydrophobic substrate and the aqueous polymerizing solution (16). Thus, in an attempt to further disrupt the PEG network structure so as to increase its permeability, we incorporated hydrophobic NPs into the hydrogel matrix. By analogy, the large interfacial zone between the hydrophobic particles and the surrounding aqueous macromonomer solution should lead to more network defects in the vicinity of the particles (Fig. 2).

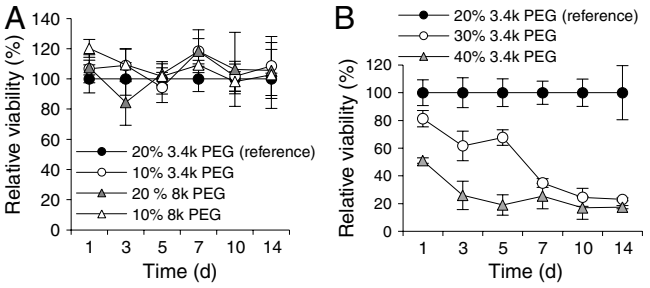

Fig. 1. (*A*) As a reference, we used 3.4 k molecular weight of PEG and prepared samples from prepolymer with 20% (wt/wt) solid content, referred to as 20% 3.4 k PEG. When samples were prepared by increasing molecular weight or reducing solid content from 20% 3.4 k PEG, there were no significant changes in the viability of encapsulated cells compared with 20% 3.4 k PEG (p value = 0.32). (*B*) However, there were significant cell viability drops from 20% 3.4 k PEG to 30% 3.4 k PEG (p value < 0.01), from 30% 3.4 k PEG to 40% 3.4 k PEG (p value < 0.01).

We first evaluated whether the incorporated hydrophobic NPs would indeed augment network defects and improve permeability. We selected PLGA as a suitable hydrophobic material for the particle because of its biocompatibility (17). When hydrophobic NPs (870 ± 34 nm diameter) were incorporated into PEG matrices (0.01% wt/vol) without cells, we observed reduced mechanical strength (Fig. 3*A*), suggesting that the level of network defects had increased; however, no change was observed when hydrophilic NPs (carboxylated polystyrene, 785 ± 6 nm diameter) were added (Fig. 3*A*). Because albumin (14 nm × 4 nm × 4 nm dimensions) is known to be an effective marker to probe effective network sizes (15), we also compared albumin release from samples containing hydrophobic NPs with release results for samples containing hydrophilic NPs. We observed that only hydrophobic NPs improve the permeability of PEG matrices (Fig. 3*B*); no such effect was observed for hydrophilic NP-containing samples (Fig. 3*B*).

We then incorporated PLGA NPs into cell-encapsulating PEG matrices. Fig. 3*C* depicts Huh 7.5 cells encapsulated in PEG matrices with and without NPs. Cell viability was increased for all the different thicknesses of PLGA NP-containing samples, as shown in Fig. 3*D*. The increase of cell viability in proportion to the matrix thickness implies that the dominant benefit from addition of PLGA NPs is the improvement in permeability. We also evaluated the effects of different conditions of NPs, including hydrophobicity/hydrophilicity, size, concentration, and PLGA composition (Fig. S1). These studies demonstrated that the presence of hydrophobicity of PLGA NPs is the primary factor contributing to the improvement in encapsulated cell viability. Fig. 3*E* shows a significant increase in the live cell population (green fluorescence) and in the number of cell colonies (white arrows) for the PLGA NP-containing samples, as stained by the Live/Dead® viability measurement kit. The formation of cell colonies is important for hepatic cells to function normally because of their dependence on cellular interactions. Thus, our network design provides a more desirable environment for encapsulated cells to proliferate and restore homotypic cellular interactions.

In the preceding experiments studying various encapsulating conditions, we mainly used Huh 7.5, a hepatoma cell, which is widely used in HCV research to overcome the limited ability of other liver-derived cells to support HCV replication, in vitro (18). One problem is that it is typically difficult to maintain primary human hepatocytes in standard 2D in vitro cultures in which they rapidly lose features of advanced differentiation (19). There has been an attempt to encapsulate rat primary hepatocytes in PEG matrices, but the viability was too poor to perform biological assays (20). Thus, there needs to be a better cell-encapsulation system for the 3D culture of primary hepatocytes in order to fully benefit from the potential advantages offered by PEG hydrogels. Because of the resistance to cell attachment to the PEG network and the anchor dependence of liver-derived cells, we conjugated RGD (Arg-Gly-Asp) peptides, a cell binding domain (21), to the PEG network for human primary hepatocyte encapsulation. To test the benefit of incorporating PLGA NPs, we measured the viabilities of different sample groups. As expected, there were significant improvements in viability for NP-containing samples (Fig. 4*A*).

Because our approach was designed to improve phenotype stability by increasing matrix permeability, we selected urea as a hepatic function marker because the diameter (less than 0.5 nm) is small enough not to be trapped by the network. We verified that there was no significant difference in urea diffusion between samples with and without PLGA NPs (Fig. S2). As expected, we observed significant increases in urea secretion, normalized by each sample's viability, in the samples with PLGA NPs (Fig. 4*B*).

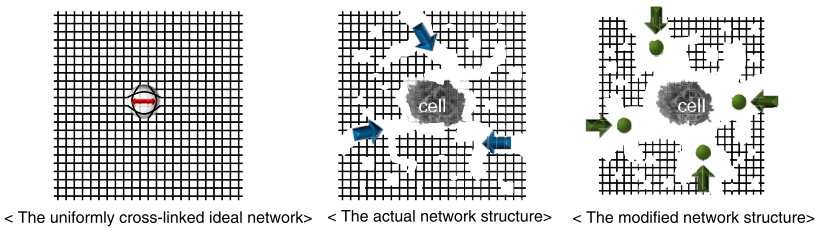

Fig. 2. The distance between consecutive cross-links (red arrow) controls the permeability of polymeric networks only in the case when the network is uniformly cross-linked. However, under the curing condition that was optimized cell-encapsulating PEG networks, there are numerous network defects (blue arrows), which appear to be up to orders of magnitude larger than the possible range of distances between consecutive cross-links. Therefore, the level of these network defects is the primary determinant of the hydrogel permeability and its consequent ability to support metabolic activities of encapsulated cells. These network defects could be augmented by the incorporation of hydrophobic NPs (green circles), which are believed to induce even looser cross-linking within the hydrophilic PEG network.

We also measured the induction activity of cytochrome P-450 monooxygenase 3A4 (CYP3A4). CYP3A4 is involved in the oxidative metabolism of various xenobiotics, including more than 50% of clinically used drugs (22). The expression level of this enzyme is related to the accumulation of toxic metabolites, drug side effects, and the therapeutic efficacy of a coadministered drug (23). The induction activity of CYP3A4 was evaluated by the relative expression level of the enzyme between samples cultured with and without inducers, which avoids permeability effects between samples. We tested induction of CYP3A4 activity to rifampicin, a bactericidal antibiotic drug of the rifamycin group, which is known to be one of the most reliable CYP3A4 inducers (24). We used human adult primary hepatocytes from two donors that had lost the CYP3A4 induction activity when they were cultured on collagen-coated 2D tissue culture plates (Fig. 4*C*). Even though the cells in 3D matrices without NPs showed no response to the inducer (Fig. 4*C*), we observed restored induction activity of CYP3A4 in NP-containing samples (Fig. 4*C*). Taken together, these results show that incorporation of hydrophobic NPs is an effective way to improve phenotype stability of encapsulated cells.

New Network Design Maintains Patternability of Cell-Encapsulating PEG Hydrogels. One of the critical features of engineered tissue scaffolds is the replication of in vivo geometry and dimensional size scale in order to provide an environment that could potentially guide cell behavior with respect to morphology, cytoskeletal structure, and functionality (25). In order to obtain more reliable microscale architectures within a PEG matrix, there should be appropriate mechanical strength for long-term structural stability, and the viscosity of the fluid prepolymer needs to be low enough for the prepolymer to flow into microscale mold structures to allow fabrication through soft lithography or microfluidic processing. However, because the diffusion condition in PEG-based scaffolds is the primary factor for phenotype stability of encapsulated cells, it is a challenge to design a network to satisfy these contradictory requirements. Because our network design for improving the hydrogel permeability was intended to partially induce loose cross-linking only at the particle-PEG interface,

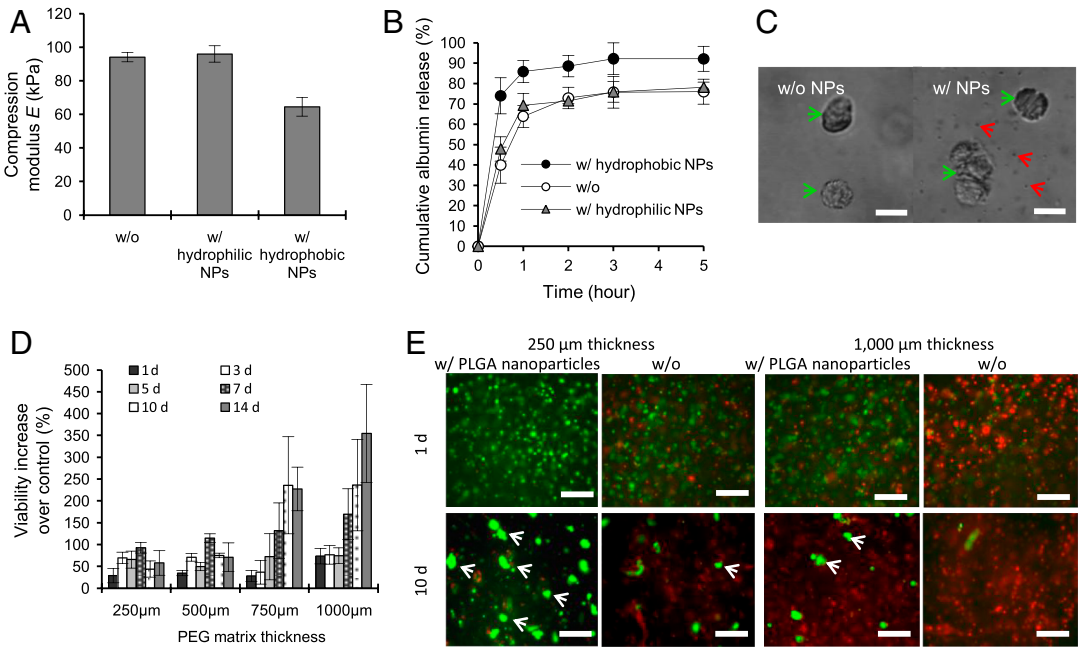

Fig. 3. (*A*) Compression modulus of PEG matrices without NPs, with hydrophilic NPs (polystyrene beads with carboxylated surfaces), or with hydrophobic PLGA NPs were measured, and only hydrophobic NP-containing samples had reduced compression modulus (p value < 0.01). (*B*) When albumin was encapsulated in PEG matrices without cells, samples containing hydrophobic PLGA NPs showed significantly improved albumin release, (p value < 0.01), whereas hydrophilic NPs had no effect on release profiles (p value = 0.57), compared with samples without NPs. (*C*) PLGA NPs (red arrows) were incorporated within matrices encapsulating Huh 7.5 cells (green arrows). Scale bar: 10 μm. (*D*) For different thicknesses of PLGA NP-containing samples, increased cell viabilities were observed compared to samples without NPs. (*E*) The improved viabilities in NP-containing samples are shown in the figures stained by Live/Dead® assay (green: live cells; red: dead cells). White arrows indicate cell colonies resulting from proliferation of individual cells. Scale bar: 100 μm.

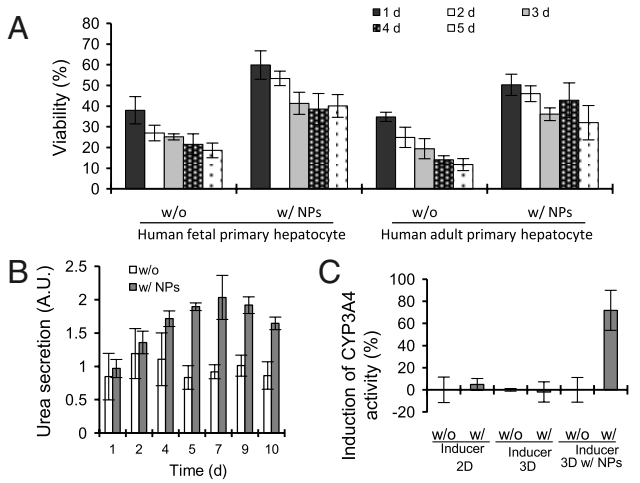

Fig. 4. (*A*) The addition of PLGA NPs led to further improvement of the viability of human fetal primary hepatocytes (p value < 0.01) and human adult primary hepatocytes (p value < 0.01). (*The viability represents "live cell number relative to the number of initially encapsulated cells.") (*B*) Urea secretion from human adult primary hepatocytes was used as a hepatic function marker and normalized by cell viability. Increases in normalized urea secretion were observed for PLGA NP-incorporated samples (p value < 0.01). (*C*) The CYP3A4 expression levels of human adult primary hepatocytes were measured and normalized by each sample's viability. Induction of CYP3A4 activity of human adult primary hepatocytes was lost for 2D (cultured on collagen-coated plates with 100% confluency, p value = 0.092) and 3D samples without NPs (encapsulated in PEG hydrogels without PLGA NPs, p value = 0.73). However, there was significant restoration of the induction of CYP3A4 activity in 3D samples with NPs (encapsulated in PLGA nanoparticle-incorporated hydrogels, p value < 0.01).

we anticipated that this approach would also minimize loss of physical properties for patternability.

In order to evaluate the physical characteristics necessary to patternability, we measured the viscosity of the prepolymer and compression modulus of the cured matrices. As the macromonomer molecular weight increased from 3.4 k to 8 k, the viscosity increased ($306 \pm 3\%$) and the compression modulus of the cured gel decreased ($77 \pm 4\%$), as shown in Fig. 5*A*. Because 8 k PEG matrices had similar cell viability as for 3.4 k PEG matrices, as shown in Fig. 1*A* the ideal network mesh size was not an appropriate design parameter. PLGA NP-containing samples showed no significant change in the viscosity of the prepolymer solution (p value > 0.05) and only modest loss in the gel compression modulus ($31 \pm 3\%$) (Fig. 5*A*). The ability to support increased cell viability while maintaining patternability opens the door to developing hydrogel platforms with more sophisticated architectures that promote phenotype stability for different primary cell types.

Ultimately, one condition for phenotype stability is simply high cell viability. With this in mind, one notable feature of the Huh 7.5 cells encapsulated in the reference PEG matrices—initially used to optimize cell encapsulation conditions—is that the cell viability was always greater at the edges of the hydrogel matrix than in the middle portion, as reported for rat hepatocytes (13) and human mesenchymal stem cells (26). Because cells require the diffusion of nutrients, oxygen, and waste by-products through the PEG matrix to support their metabolic activities, we hypothesized that lower cell viability in the middle portion was caused by insufficient permeability of the PEG hydrogel. This correlation between cell viability and matrix permeability was confirmed by the observation that increasing the thickness of the PEG hydrogel led to decreased viabilities in both Huh 7.5 cells and human fetal

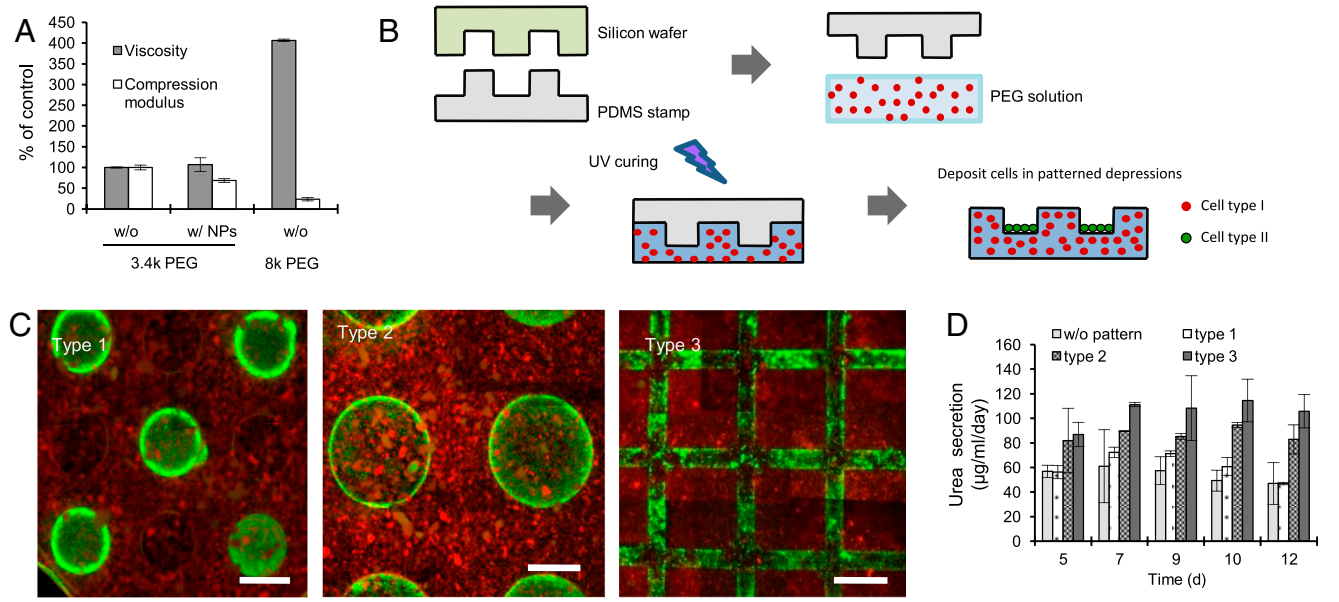

Fig. 5. (*A*) The addition of PLGA NPs had no significant effect on viscosity of aqueous 20% 3.4 k PEG solution (p value = 0.51), whereas 20% 8 k PEG had $306 \pm 3\%$ higher viscosity than 20% 3.4 k PEG. Samples containing NPs had $31 \pm 3\%$ reduced compression modulus compared to samples without NPs, whereas samples prepared with 8 k PEG had $77 \pm 4\%$ reduced compression modulus compared to samples prepared with 3.4 k PEG. (*B*) Schematic illustration of cell patterning process. Microstructures were fabricated in a silicon wafer by standard microfabrication techniques and then transferred to a PDMS replica. The PEG prepolymer with cells was cured between a glass slide and the PDMS replica. Another type of cell was loaded on the surface, and they were trapped into the patterned depressions by mild agitation or flow. (*C*) Fluorescence images of encapsulated cells (red) in PEG matrices and patterned cells (green) on the surface. Hepatocytes and fibroblasts were encapsulated following 2-d coculturing on cell culture dishes, and fibroblasts were loaded in the patterned depressions on the surface. All samples had the same number of encapsulated hepatocytes and fibroblasts. Type 2 and Type 3 had twice the number of fibroblasts on the surface than Type 1. Scale bar: 1.000 μm (*D*) As more fibroblasts on the surfaces were loaded from samples without fibroblasts to sample Type 2, urea secretions increased (p value < 0.01, regression analysis). Type 3 had greater urea secretion than Type 2 (p value < 0.01), even though both had the same number of fibroblasts on the surface. All statistical analyses in *D* were done after a stabilization period (from 5 d after encapsulation).

primary hepatocytes (Fig. S3). Thus, patternability can be potentially exploited to further increase cell viability.

Herein, however, we primarily focused on controlling the spatial distribution of incorporated cells within cell-encapsulating PEG in order to demonstrate the potential of our system for replicating tissue microarchitectures. In many tissues, different types of cells distribute with specific configurations, and their interactions are of fundamental importance in physiology, pathophysiology, oncology, developmental biology, and wound healing (27). In the actual liver, for example, hepatocytes are aggregated in sheets and separated by blood channels, called sinusoids. The proper distribution of nonparenchymal cells along the sinusoid is a prerequisite to restore various functions of the liver (28). Several approaches have been successfully proposed to restore heterotypic interactions (29).

We sought a method to guide cells' spatial displacement with a simplified patterning process, which is given in Fig. 5*B*, as proof of the principle. The patterning process did not hinder cell viability (Fig. S4). Indeed, due to the minimal loss of mechanical strength, the patterned structure was maintained for more than 1 mo. The microstructure was designed to control the spatial distribution of encapsulated cells and to trap other types of cells within the patterned, depressed regions on the surface of cell-encapsulating PEG matrices (Fig. 5*C*). Because the incorporation of hydrophobic NPs was verified to improve homotypic interactions, we reasoned that we might be able to achieve an even more desirable 3D environment for the encapsulated cells by providing a second cell type on the surface, thus providing both homotypic and heterotypic cellular interactions, as present in many tissues. Because cellular interaction between hepatocytes and fibroblasts has been well-investigated and is known to enhance hepatic functions (27), we selected fibroblasts for incorporation into our system. It has been reported that cellular interactions between hepatocytes and fibroblasts are initiated only by direct contact-mediated signals, but they could be maintained within a short range (~325 μm) by soluble signals (30). Thus, even after the fibroblasts had been exchanged with naive fibroblasts that had not been in direct contact with hepatocytes, the hepatocytes could conceivably maintain the initiated interaction with the naive fibroblasts by soluble signals (30). In order for encapsulated hepatocytes to interact with fibroblasts on the matrix surface, we first cocultured human adult primary hepatocytes with NIH 3T3 fibroblasts for 2 d and encapsulated both cell types into PEG matrices. Then NIH 3T3 fibroblasts were loaded on the matrix surface. Because we had verified that increased interaction with fibroblasts led to increased secretion of urea and albumin from hepatocytes (Fig. S5), the cellular interaction between encapsulated hepatocytes and fibroblasts on the matrix surface could be evaluated by the secreted amounts of these hepatic function markers. In our system, the cellular interaction between two types of cells could be reliably regulated by controlling cell numbers on the matrix surface at specific configurations. In Fig. 5*C*, all samples had the same number of encapsulated hepatocytes and fibroblasts, and Type 2 and Type 3 configurations had twice as many fibroblasts on the surface compared to the Type 1 configuration.

As reported in other work (27), it took several days for the two types of cells to establish stable heterotypic interactions, so we waited 5 d after encapsulation before we started examining the secretion of hepatic markers. As expected, increased numbers of fibroblasts on the matrix surface led to enhanced secretion of urea, as shown in comparison between samples without fibroblasts on the matrix surface vs. sample Type 1 (Fig. 5*D*, p value $<$ 0.05), and for Type 1 vs. Type 2 (Fig. 5*D*, p value $<$ 0.01). We also observed that different configurations of patterned cells on the matrix surface resulted in different levels of urea secretion, as shown in comparison of Type 2 and Type 3 (Fig. 5*D*, p value $<$ 0.01). Because the interaction between encapsulated hepatocytes and fibroblasts was mediated by soluble signals, we suggest that the increased urea secretion for Type 3 compared to Type 2 could be due to a more favorable surface configuration in Type 3, in which fibroblasts were well-distributed over the surface so that soluble signals could be delivered to more encapsulated cells. Even though this experiment was designed only to provide a qualitative evaluation of heterotypic interactions, this approach provides a platform to understand how distributions of different types of cells and their consequent interactions affect various biological responses.

In summary, we first suggested that network defects serve as an important parameter in modifying the physical configuration of the cell-encapsulating PEG network. Based on this hypothesis, we incorporated hydrophobic NPs to augment network defects by purposefully inducing loose cross-linking at the particle-PEG interface. This approach was verified to be an effective way to satisfy the seemingly contradictory requirements for an optimal network; it improved the permeability to support metabolic activities of cell-encapsulating PEG matrices while maintaining patternability by minimizing the loss of mechanical strength and viscosity. This structural advantage allowed us to construct micron-scale cell-trapping architectures for the encapsulated cells to potentially restore heterotypic cellular interactions more akin to native tissues. We expect that this strategy to design network structures of cell-encapsulating hydrogels can be applied to restore more natural 3D environments of many tissues with complicated architectures.

Materials and Methods

Additional Materials and Methods are provided in *SI Materials and Methods*.

Preparation of Hydrophobic Particles of PLGA. A solution of 1% (wt/vol) 50/50 PLGA (composed of 50/50 molar ratio of glycolide units and lactide units, 85 k molecular weight, LACTEL) in dichloromethane (DCM, Sigma-Aldrich) was poured into 100 times its volume of water. The solution was emulsified for 2 min at ~30,000 rpm using a PRO200 Laboratory Homogenizer (Pro Scientific). The emulsion was stirred at 1,000 rpm overnight at room temperature and atmospheric pressure to allow DCM to evaporate. The particle suspension was separated by centrifugation and placed in a vacuum desiccator overnight. The average diameter of the NPs, measured by dynamic light scattering, was 870 ± 34 nm.

Cell Encapsulation in PEG Matrices. PEG diacrylate (PEG-DA) was dissolved in PBS with 0.05% (wt/vol) of the photoinitiator, Irgacure 2959 (Ciba). Hydrophobic PLGA NPs were added to the solution for some samples with the designated concentrations. For hydrophilic particles, we used 785 ± 6 nm diameter polystyrene beads (Polybead® Carboxylate 0.75 Micron Microspheres, Polysciences) that had been surface-modified with carboxyl groups. The cell suspension was then added to a given PEG-DA prepolymer solution at 10×10^6 cells/mL for Huh 7.5 cells and 30×10^6 cells/mL for human primary hepatocytes. For primary hepatocyte encapsulation, RGD-conjugated PEG was mixed with the prepolymer at 20 μmol/mL. The final prepolymer solution was loaded between glass slides (VWR) separated by a Teflon spacer and exposed to 320–390 nm UV light with 10 mW/cm^2 intensity (Cure spot 50, DYMAX) for 50 s. The cured hydrogels were subsequently washed with PBS and then cultured in ultralow attachment multiwell plates (Corning) with cell culture medium; the medium was changed every 2 d. For primary hepatocyte encapsulation, RGD-conjugated PEG was mixed with the prepolymer at 20 μmol/mL. Note that the curing conditions for cell-encapsulating PEG matrices involved reducing the photoinitiator concentration, UV exposure time, and UV intensity for better cell viability as compared to samples prepared under much more complete curing conditions used in our previous study (31).

Cell Patterning Within Cell-Encapsulating PEG Matrices. Microstructures in silicon wafers were prepared by standard microfabrication processing techniques. We created structures 200 μm deep by using the Surface Technology Systems Deep RIE Etcher. The microstructures could be transferred to poly (dimethylsiloxane) (PDMS) replicas by curing PDMS prepolymer (SYLGARD® 184 Silicone Elastomer kit, Dow Corning Corporation) for 30 min at 70 °C over the silicon wafer. Cell-containing PEG prepolymer was cured between the PDMS replicas and a glass slide. The second type of cells was loaded within the microstructure on the PEG matrix surface. By generating slight agitation or flow, loaded cells were stably entrapped within the patterned depressions

where less shear stress was applied. After allowing 1 h for cells to attach on the surface of RGD-conjugated PEG matrices, unattached cells were removed by rinsing with cell culture media, and the matrices were incubated under normal cell culturing conditions. To obtain images of patterned cells, encapsulated cells were stained red by DiI (Vybrant™ Cell-Labeling Solutions, Molecular Probes®), and patterned cells were stained green by DiO (Vybrant™ Cell-Labeling Solutions, Molecular Probes®).

Statistical Analysis. All measurements in this manuscript were repeated at least two times to confirm the reproducibility. Experiments done with Huh 7.5 cells had $n \geq 6$, and experiments done with human primary hepatocytes had $n \geq 3$. Statistical analysis was performed by One-way ANOVA with Bonferroni–Holm post hoc test through overall time points. Regression analysis was performed through overall time points with average values of each sample. All values are reported as the mean and standard deviation of the mean.

ACKNOWLEDGMENTS. The authors gratefully acknowledge the graduate fellowship of the Mogam Scientific Scholarship (to W.L.), the American Liver Foundation Postdoctoral Fellowship Award and a Stanford Dean's Postdoctoral Fellowship (to N.-J.C.), a Beckman Interdisciplinary Translational Research Program Award, a Burroughs Welcome Fund Clinical Scientist Award in Translational Research (to J.S.G.), the Center for Translational Research in Chronic Viral Infections, the Center on Polymer Interfaces and Macromolecular Assemblies, and a National Science Foundation Materials Research Science and Engineering Center.

1. Hubbell JA (1995) Biomaterials in tissue engineering. *Nat Biotechnol* 13:565–576.
2. Cushing MC, Anseth KS (2007) Hydrogel cell cultures. *Science* 316:1133–1134.
3. Langer R, Vacanti JP (1993) Tissue engineering. *Science* 260:920–926.
4. Jhon MS, Andrade JD (1973) Water and hydrogels. *J Biomed Mater Res* 7:509–522.
5. Sawhney AS, Pathak CP, Hubbell JA (1993) Interfacial photopolymerization of poly(ethylene glycol)-based hydrogels upon alginate-poly(l-lysine) microcapsules for enhanced biocompatibility. *Biomaterials* 14:1008–1016.
6. Drury JL, Mooney DJ (2003) Hydrogels for tissue engineering: scaffold design variables and applications. *Biomaterials* 24:4337–4351.
7. Khademhosseini A, Langer R, Borenstein J, Vacanti JP (2006) Microscale technologies for tissue engineering and biology. *Proc Natl Acad Sci USA* 103:2480–2487.
8. Sachlos E, Czernuszka JT (2003) Making tissue engineering scaffolds work. Review: The application of solid freeform fabrication technology to the production of tissue engineering scaffolds. *Eur Cells Mater* 5:29–39.
9. Lee KY, Mooney DJ (2001) Hydrogels for tissue engineering. *Chem Rev* 101:1869–1880.
10. de Gennes PG (1979) *Scaling Concepts in Polymer Physics* (Cornell Univ Press, Ithica, NY).
11. Cruise GM, et al. (1999) In vitro and in vivo performance of porcine islets encapsulated in interfacially photopolymerized poly (ethylene glycol) diacrylate membranes. *Cell Transplant* 8:293–306.
12. Cho NJ, et al. (2009) Viral infection of human progenitor and liver-derived cells encapsulated in three-dimensional PEG-based hydrogel. *Biomed Mater* 4:11001–11007.
13. Tsang VL, et al. (2007) Fabrication of 3D hepatic tissues by additive photopatterning of cellular hydrogels. *FASEB J* 21:790–801.
14. Cruise GM, Scharp DS, Hubbell JA (1998) Characterization of permeability and network structure of interfacially photopolymerized poly(ethylene glycol) diacrylate hydrogels. *Biomaterials* 19:1287–1294.
15. Gong JP, et al. (2001) Synthesis of hydrogels with extremely low surface friction. *J Am Chem Soc* 123:5582–5583.
16. Gong JP, Kii A, Xu J, Hattori Y, Osada Y (2001) A possible mechanism for the substrate effect on hydrogel formation. *J Phys Chem B* 105:4572–4576.
17. Lee W, Wiseman ME, Cho NJ, Glenn JS, Frank CW (2009) The reliable targeting of specific drug release profiles by integrating arrays of different albumin-encapsulated microsphere types. *Biomaterials* 30:6648–6654.
18. Blight KJ, McKeating JA, Rice CM (2002) Highly permissive cell lines for subgenomic and genomic hepatitis C virus RNA replication. *J Virol* 76:13001–13014.
19. Maher JJ (1988) Primary hepatocyte culture: Is it home away from home? *Hepatology* 8:1162–1166.
20. Underhill GH, Chen AA, Albrecht DR, Bhatia SN (2007) Assessment of hepatocellular function within PEG hydrogels. *Biomaterials* 28:256–270.
21. Ruoslahti E, Pierschbacher MD (1986) Arg-Gly-Asp: A versatile cell recognition signal. *Cell* 44:517–518.
22. Lehmann JM, et al. (1998) The human orphan nuclear receptor PXR is activated by compounds that regulate CYP3A4 gene expression and cause drug interactions. *J Clin Invest* 102:1016–1023.
23. Moore LB, et al. (2000) Orphan nuclear receptors constitutive androstane receptor and pregnane X receptor share xenobiotic and steroid ligands. *J Biol Chem* 275:15122–15127.
24. Bachmann KA, Jauregui L (1993) Use of single sample clearance estimates of cytochrome P450 substrates to characterize human hepatic CYP status in vivo. *Xenobiotica* 23:307–315.
25. Desai TA (2000) Micro-and nanoscale structures for tissue engineering constructs. *Med Eng Phys* 22:595–606.
26. Nuttelman CR, Tripodi MC, Anseth KS (2004) In vitro osteogenic differentiation of human mesenchymal stem cells photoencapsulated in PEG hydrogels. *J Biomed Mater Res* 68:773–782.
27. Bhatia SN, Balis UJ, Yarmush ML, Toner M (1999) Effect of cell-cell interactions in preservation of cellular phenotype: Cocultivation of hepatocytes and nonparenchymal cells. *FASEB J* 13:1883–1900.
28. Jungermann K, Keitzmann T (1996) Zonation of parenchymal and nonparenchymal metabolism in liver. *Annu Rev Nutr* 16:179–203.
29. Andersson H, Berg A (2004) Microfabrication and microfluidics for tissue engineering: state of the art and future opportunities. *Lab Chip* 4:98–103.
30. Hui EE, Bhatia SN (2007) Micromechanical control of cell–cell interactions. *Proc Natl Acad Sci USA* 104:5722–5726.
31. Myung D, et al. (2008) Glucose-permeable interpenetrating polymer network hydrogels for corneal implant applications: A pilot study. *Curr Eye Res* 33:29–43.